colloids and interfaces

MDPI

Article

Alginate Films Encapsulating Lemongrass Essential Oil as Affected by Spray Calcium Application

Martina Cofelice [1,*], Francesca Cuomo [1] and Amparo Chiralt [2,*]

[1] Department of Agricultural, Environmental and Food Sciences (DiAAA) and Center for Colloid and Surface Science (CSGI), University of Molise, Via De Sanctis, I-86100 Campobasso, Italy

[2] Instituto Universitario de Ingeniería de Alimentos para el Desarrollo, Universitat Politècnica de València (UPV), Camino de Vera s/n, 46022, Valencia, Spain

* Correspondence: m.cofelice1@studenti.unimol.it (M.C.); dchiralt@tal.upv.es (A.C.)

Received: 1 August 2019; Accepted: 3 September 2019; Published: 4 September 2019

Abstract: The necessity of producing innovative packaging systems has directed the attention of food industries towards the use of biodegradable polymers for developing new films able to protect foods and to extend their shelf-life, with lower environmental impact. In particular, edible films combining hydrophilic and hydrophobic ingredients could retard moisture loss, gas migration and ensure food integrity, reducing the necessity of using synthetic plastics. Alginate-based films obtained from emulsions of lemongrass essential oil (at 0.1% and 0.5%) in aqueous alginate solutions (1%), with Tween 80 as surfactant (0.3%), were obtained by casting and characterized as to microstructure and thermal behavior, as well as tensile, barrier and optical properties. Films were also crosslinked through spraying calcium chloride onto the film surface and the influence of oil emulsification and the crosslinking effect on the final film properties were evaluated. The film microstructure, analyzed through Field Emission Scanning Electron Microscopy (FESEM) revealed discontinuities in films containing essential oil associated with droplet flocculation and coalescence during drying, while calcium diffusion into the matrix was enhanced. The presence of essential oil reduced the film stiffness whereas calcium addition lowered the film's water solubility, increasing tensile strength and reducing the extensibility coherent with its crosslinking effect.

Keywords: alginate; calcium crosslinking; edible films; lemongrass essential oil

1. Introduction

One of the interests of the food industries is to extend the shelf-life of food products through new strategies, such as the improvement of edible films by means of antimicrobial compounds, antioxidants or molecules that could modify the physical characteristics according to the requirements of the different food products [1].

Previous generations of packaging systems were mainly based on petroleum plastic materials associated with serious environmental drawbacks [2]. Nowadays, their composition is being replaced by biodegradable materials, such as alginate, chitosan, pectin, starch, milk proteins, etc., thus making the packaging a biocompatible and/or edible element [3]. Edible films and coatings are two forms of packaging assembled following different routes. The former are pre-formed wrapping layers that can be used to pack food products separately and the latter are thin layers tightly adhering to the food surface and generally formed on it [4]. Edible films, as well as the traditional films, have specific functions, such as retarding moisture loss and gas migration, ensuring food integrity or retaining flavor [5]. The components of these films are edible ingredients, such as hydrocolloids and lipids, used alone or in combination to form a thin layer in order to protect food and prolong its shelf life. Of the hydrocolloids, alginate is a natural polymer that can be used for the production of edible

coatings and films [6]. It is isolated from different species of brown seaweeds and is a linear polysaccharide where guluronic (G) and mannuronic (M) acids are the constituting monomers, present in different ratios. Anionic, water-soluble, biocompatible, food-grade and low cost, alginate meets the requisites of application in several fields, also exhibiting interesting rheological properties [7,8]. Alginate is also used as a thickening or gelling agent in food formulations, demonstrating its ability to react with divalent cations (like calcium) to form a strong network [9].

Of the hydrophobic compounds, essential oils (EOs), which are aromatic liquids obtained from plants, are widely accepted by consumers because they are perceived as natural products. Additionally, many of the essential oil compounds exhibit antioxidant and antimicrobial properties, and can replace chemical preservatives in foods [10]. Moreover, due to their lipid nature, they could solubilize functional lipophilic molecules. The good mechanical properties of the natural polysaccharides and the interesting functional aspects of EOs can be held together, through emulsification, in a matrix successively used to form films with improved physicochemical features, while the EOs provide the films with antioxidant and antimicrobial properties for food preservation [11]. Of the EOs, lemongrass essential oil (LEO) exhibited antimicrobial activity against *E. coli* and *S. aureus*, when encapsulated in nanocapsules of polylactic acid, and also against *Botritis cynerea* [12,13]. When incorporated in edible coating, LEO prolonged the shelf life of different fresh-cut fruits, such as pineapples and apples [14,15].

The aim of this study was to analyze the physicochemical behavior of alginate films formed from emulsions of LEO in alginate solutions, stabilized by non-ionic surfactant Tween 80. The films were subjected, or not, to a crosslinking with calcium chloride applied through spray, in order to simulate an in-line process when the film-forming solutions are used as food coatings and calcium can be subsequently applied by spraying the coated surface. In particular, four film-forming formulations have been used to evaluate how film properties are influenced by the presence of surfactant and LEO (at low and high concentrations) and the effect of the crosslinking agent in each case.

2. Materials and Methods

2.1. Materials

Food-grade sodium alginate was obtained from Farmalabor (Canosa di Puglia, Italy), Tween 80 (Polyoxyethylene (20) sorbitan monooleate), non-ionic surface active agent (T), and Lemongrass Essential Oil (LEO) were purchased from Sigma-Aldrich (Madrid, Spain). Calcium chloride, $Mg(NO_3)_2$ and P_2O_5 were supplied by Panreac Química, S.A. (Castellar del Vallés, Barcelona, Spain). For all the preparations ultra-pure water was used.

2.2. Emulsion Preparation and Characterization

Primary emulsions were obtained, according to previous studies [7,9], by mixing LEO (0.5–2.5% w/w) as lipidic phase and Tween 80 (1.5% w/w) as surface active agent in an aqueous suspension of sodium alginate (1% w/w) with a laboratory T25 digital Ultra-Turrax rotor-stator homogenizer (S25-N25 - IKA, Staufen, Germany) at 20,000 rpm for 4 min. The obtained dispersions were then subjected to ultrasonic treatment (Vibra Cell, Sonics & Materials, Inc. USA) for 20 min at 40% amplitude with pulses of 1 s. A suspension containing only Tween 80 (1.5% w/w) and alginate (1% w/w) was prepared in order to evaluate the influence of the surfactant on the studied properties. Emulsions were characterized as to the particle size of the dispersed phase, the polydispersity index (PDI) and ζ-potential through a Zetasizer Nano instrument (Malvern Instruments Ltd., Worcestershire, UK) using a HeNe laser at 633 nm and a detector with scattering angle at 173°. Samples were first diluted with ultra-pure water to prevent multiple scattering effects. Particle size was determined at 25 °C after 120 s of equilibration time. The ζ-potential of samples was measured using a specific cuvette (DTS1070) and the Smoluchowski model was selected to analyze the recorded data.

2.3. Film Preparation

Solutions of sodium alginate were obtained by dissolving the polymer (1% w/w) in hot water at 70 °C under continuous stirring. Film-forming dispersions (FFDs) with LEO were also prepared by mixing the primary emulsions or the surfactant dispersion into the alginate solution to obtain a final concentration of LEO of 0%, 0.1% (low content) and 0.5% (high content) w/w. In order to form polymer films, a known amount of each formulation was spread onto Teflon disks (diameter 15 cm) to have 1 g of polymer per plate. Films were left to dry at room temperature at a relative humidity (RH) of 45–50%. Prior to testing, films were equilibrated at 25 °C in desiccators containing a saturated solution of $Mg(NO_3)_2$ (53% RH).

Film crosslinking was carried out by spraying the film surface with a solution of $CaCl_2$ 0.1 M. The solution was applied through an airbrush (model E4182, Elite pro) equipped with a 0.8 mm nozzle, onto the surface of the film for 1 minute considering a flow of about 6 mL/min. The plate was rotated 90° during the application of the calcium chloride solution to cover the film surface uniformly as shown in Figure 1. The application of calcium was carried out when the FFDs were partially dried (about 60% weight loss). Once sprayed, the films were left to complete the drying process in the same conditions as mentioned above, then peeled and equilibrated. All the sample codes and compositions are given in Table 1.

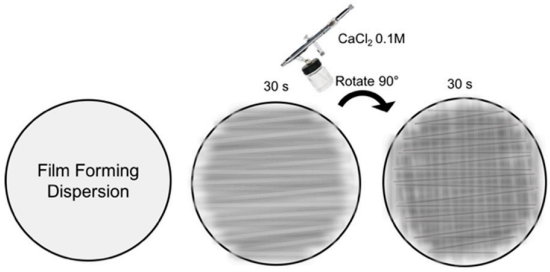

Figure 1. Representation of the application of calcium chloride solution on films through spaying.

Table 1. Sample codes, composition and nominal mass fraction (X) of different components in the dried films.

Sample	Composition	X_A	X_{T80}	X_{CaCl_2}	X_{LEO}
A	Alginate	1.00			
A-Ca	Alginate + $CaCl_2$	0.92		0.081	
A-T	Alginate-Tween 80	0.77	0.23		
A-T-Ca	Alginate-Tween 80 + $CaCl_2$	0.72	0.22	0.063	
A-T-LEO L	Alginate-Tween 80-LEO Low	0.71	0.21		0.072
A-T-LEO L-Ca	Alginate-Tween 80-LEO Low + $CaCl_2$	0.67	0.20	0.059	0.067
A-T-LEO H	Alginate-Tween 80-LEO High	0.55	0.17		0.279
A-T-LEO H-Ca	Alginate-Tween 80-LEO High + $CaCl_2$	0.53	0.16	0.046	0.266

X_A fractional mass of alginate, X_{T80} fractional mass of Tween 80, X_{CaCl_2} fractional mass of calcium chloride incorporated by spraying, X_{LEO} fractional mass of Lemongrass Essential Oil.

2.4. Film Characterization

2.4.1. Film Microstructure

For the microstructural analysis, samples were conditioned in desiccators containing P_2O_5 in order to eliminate the water content. Then the films without calcium were immersed in liquid nitrogen to obtain cryofractured cross-sections [16] while the film treated with calcium were partially fractured with a scalpel to avoid the separation of the different lamina. After that, the samples were mounted on copper stubs and covered with platinum. Images were obtained by Field Emission

Scanning Electron Microscopy (FESEM) (ZEISS®, model ULTRA 55, Germany), using an accelerating voltage of 1.5 and 2 kV.

2.4.2. Film Thickness

The film thickness was measured using a digital electronic micrometer (Palmer, COMECTA, Barcelona, Spain) to the nearest 0.001 mm. Six measurements were taken on each tensile testing sample along the length of the strip, as well as six measurements for water vapor permeability samples. Means were used for the tensile strength (TS) and water vapor permeability (WVP) calculations, respectively.

2.4.3. Mechanical Properties

A universal test Machine (TA.XT plus model, Stable Micro Systems, Haslemere, England) was used to determine the tensile properties of films using the ASTM standard method D882 [17]. Film samples (2.5 cm wide and 10 cm long), conditioned at 25 °C and 53% RH, were mounted in the film extension grips with an initial separation set at 50 mm and stretched at 0.83 mm s^{-1} until breaking. At least six replicates were obtained for each sample. The force–distance data obtained were transformed into true stress–Hencky strain curves, from which elastic modulus (EM), tensile strength (TS) and percentage of elongation at break (%E) were obtained. In particular, TS and %E were calculated using the following equations:

$$\boldsymbol{TS} = \frac{\boldsymbol{F_{max}}}{\boldsymbol{A}} \quad (1)$$

where F_{max} is the maximum load (N) needed to break the sample and A is the initial cross–sectional area (m^2) of the sample.

$$\%\boldsymbol{E} = \left(\frac{\boldsymbol{L}}{\boldsymbol{L_0}}\right) \cdot \mathbf{100} \quad (2)$$

where L_0 is the original length of the film and L is the stretched length when the film breaks.

2.4.4. Water Vapor Permeability

The water vapor permeability (WVP) of the films was determined following a modification of the ASTM E96-95 gravimetric method [18] at 25 °C and a RH gradient of 53–100%. Payne permeability cups (3.5 cm diameter, Elcometer SPRL, Hermelle/s Argenteau, Belgium) were filled with 5 mL of distilled water (100% RH). Three circular samples of each formulation were prepared and secured to the cups with the side in contact with the Teflon plate during drying exposed to the 100% RH, attempting to simulate an application of the film on a wet surface (fresh cut fruit, vegetables). Cups were then placed in pre-equilibrated cabinets containing saturated solutions of $Mg(NO_3)_2$ to generate a RH of 53%. Each cabinet was equipped with a fan placed on the top of the cup to reduce the resistance to water vapor transport. Cups were weighed periodically at intervals of 1.5 h for 24 h after the steady state had been reached. Equation (3), reporting the water vapor transmission rate (WVTR), was used to calculate the vapor pressure on the film's inner surface (p_2) according to McHugh et al. [19].

$$\boldsymbol{WVTR} = \frac{\boldsymbol{P \cdot D \cdot Ln}\left[\frac{(\boldsymbol{p - p_2})}{(\boldsymbol{p - p_1})}\right]}{\boldsymbol{R \cdot T \cdot \Delta z}} \quad (3)$$

where P, total pressure (atm); D, diffusivity of water through air at 25 °C (m^2 s^{-1}); R, gas law constant (82.057 × 10^{-3} m^3 atm $kmol^{-1}$ K^{-1}); T, absolute temperature (K); Δz, mean stagnant air gap height (m), considering the initial and final z values; p_1, water vapor pressure on the solution's surface (atm). Finally, the WVP of films was obtained using Equation (4), where p_3 is the pressure on the film's outer surface in the cabinet.

$$\boldsymbol{WVP} = \frac{\boldsymbol{WVTR}}{(\boldsymbol{p_2} - \boldsymbol{p_3})} \cdot \boldsymbol{thickness} \quad (4)$$

2.4.5. Moisture Content and Solubility

The moisture content of the film samples was determined by means of the gravimetric method. Three samples per formulation were considered. The water was removed using a two-step method: desiccation at 60 °C for 24 h in a vacuum oven (Vacioterm-T, JP Selecta S.A., Barcelona, Spain) and storage in desiccators with P_2O_5 until constant weight was reached. The results were expressed as g of water per 100 g of dry film. Then the film solubility in water was determined. A known mass of dried films (m_0) was immersed in 15 mL of distilled water (m_w) and left for 24 h at 25 °C. Solutions were filtered and an aliquot of the filtrate was left to dry in an oven at 60 °C for 24 h, then weighed to determine the mass ratio of soluble solids per g of water of the filtrate (m_{ss}). The solubility was calculated as the g of the soluble solid per g of the water of the filtrate (Equation (5)).

$$\%\boldsymbol{S} = \frac{\boldsymbol{m_{ss}} \cdot \boldsymbol{m_w}}{\boldsymbol{m_0}} \cdot \boldsymbol{100} \quad (5)$$

2.4.6. Thermal Analysis

To characterize the thermal stability of the films, a thermo-gravimetric analyzer (TGA/SDTA 851e, Mettler Toledo, Schwarzenbach, Switzerland) equipped with an ultra-micro-weighing scale (± 0.1 μg) was used. The analysis was performed from 25 to 600 °C at a heating rate of 10 °C/min under a nitrogen flow (10 mL/min). Approximately 3 mg of sample, previously conditioned in P_2O_5, were used in each test. Derivative thermo-gravimetric analysis (DTGA) curves were analyzed and the onset temperature (T_{onset}) and maximum degradation rate temperature were registered (T_{max}).

2.4.7. Optical Properties

The optical properties of film specimens were determined using a spectrocolorimeter CM-5 (Minolta CO, Tokyo, Japan). The measurements were taken in triplicate and the opacity was determined by applying the Kubelka–Munk theory for multiple scattering [20]. The reflection spectra of samples were obtained from 400 to 700 nm on both black (R_0) and white (R) backgrounds as well as the spectra of the white background used (R_g). From these spectra, the R_∞ (the reflectance of an infinitely thick film) and *Ti* (internal transmittance, a transparency indicator) were calculated with the following equations:

$$\boldsymbol{R_\infty} = \boldsymbol{a} - \boldsymbol{b} \quad (6)$$

$$\boldsymbol{a} = \frac{\boldsymbol{1}}{\boldsymbol{2}} \cdot \left(\boldsymbol{R} + \frac{\boldsymbol{R_0} - \boldsymbol{R} + \boldsymbol{R_g}}{\boldsymbol{R_0 R_g}} \right) \quad (7)$$

$$\boldsymbol{b} = \sqrt{\boldsymbol{a^2} - \boldsymbol{1}} \quad (8)$$

$$\boldsymbol{Ti} = \sqrt{(\boldsymbol{a} - \boldsymbol{R_0})^2 - \boldsymbol{b^2}} \quad (9)$$

The CIE L* a* b* color coordinates were obtained from R_∞ spectra using illuminant D65 and observer 10° as reference. Chroma ($\boldsymbol{C^*_{ab}}$) and hue ($\boldsymbol{h^*_{ab}}$) were also determined, as well as the whiteness index (*WI*) and total color differences (ΔE), using Equations (10)–(13):

$$\boldsymbol{C^*_{ab}} = \sqrt{\boldsymbol{a^{*2}} + \boldsymbol{b^{*2}}} \quad (10)$$

$$\boldsymbol{h^*_{ab}} = \boldsymbol{arctg}\left(\frac{\boldsymbol{b^*}}{\boldsymbol{a^*}}\right) \quad (11)$$

$$\boldsymbol{WI} = \boldsymbol{100} - \sqrt{(\boldsymbol{100} - \boldsymbol{L^*})^2 + (\boldsymbol{a^*})^2 + (\boldsymbol{b^*})^2} \quad (12)$$

$$\Delta E = \sqrt{(L^*_0 - L^*_s)^2 + (a^*_0 - a^*_s)^2 + (b^*_0 - b^*_s)^2} \quad (13)$$

where L^*_0, a^*_0 and b^*_0 are the values of alginate films, while L^*_s, a^*_s and b^*_s are the measured values of the other samples.

2.5. Statistical Analysis

An analysis of variance (ANOVA) of the obtained data was performed using Statgraphics Centurion XVI software (Manugistics Corp., Rockville, Md.). Fisher's least significant difference (LSD) procedure was used at the 95% confidence level.

3. Results and Discussion

3.1. Alginate Emulsions

Alginate primary emulsions were obtained using a solution of sodium alginate as the continuous phase and two different concentrations of EO, while the amount of surfactant was fixed in order to obtain different ratios between Tween 80 and LEO and to study whether the properties of films were affected by the different size of the dispersed phase in the starting emulsions. The size distributions of the emulsions with high (2.5% w/w) and low (0.5% w/w) oil content are compared with a suspension made of alginate and Tween 80 in Figure 2.

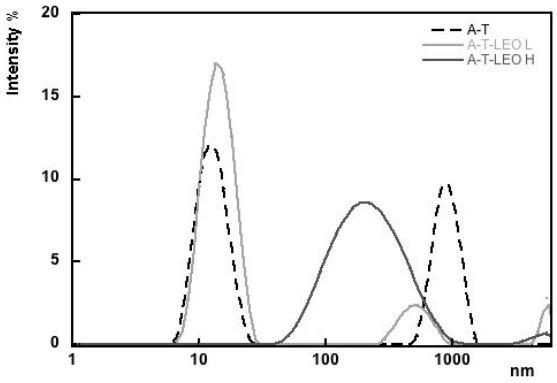

Figure 2. Particle size distribution of a suspension of alginate and Tween 80 (dashed black line), of primary alginate/lemongrass essential oil (LEO) emulsions with low (solid grey line) and high (solid black line) oil content.

As can be noted by the size distributions, formulations without LEO were characterized by a small peak around 12 nm, indicating the presence of surfactant micelles as expected, since the concentration of Tween 80 was higher than its critical micelle concentration [21], while the peak centered at 1μm was probably due to the presence of alginate aggregates (the same peak was observed for alginate suspensions—data not reported). Formulations obtained with the lower concentration of LEO were characterized by the same peak as in the absence of LEO, at 12 nm, indicating that the amount of surfactant used was enough to cover all the oil surface and to stabilize the emulsion. The (weight) ratio of surfactant to oil (SOR) is, in general, a key parameter for the production of emulsion of different sizes [22]. Specifically, the higher the SOR value, the smaller the size of the dispersed phase, and vice versa, the lower the SOR value, the greater the diameter of the dispersed phase. In this study, the emulsion with the lowest amount of LEO has a SOR of 3 and, accordingly, smaller oil droplets were observed compared to emulsions with a high oil content (2.5% LEO) and a lower SOR value, where the z-average was 158 nm. The presence of smaller or bigger droplets also influenced the visual appearance of the emulsion. The dispersions made by pure surfactant or LEO at low concentrations were transparent, while those with higher amount of oil,

characterized by droplets with a greater diameter, appeared opaque due to the different light-scattering behavior of the samples. To understand the stability of the emulsion, the ζ-potential was measured. This parameter is related to the electrokinetic potential of a particle and it is measured by evaluating its ability when interacting with a liquid surface. The determination of ζ-potential can be affected by the interaction between the particle surface and the dispersing medium by means of ionically charged functional groups present at the interface or through the adsorption of ionic species present in the medium. Values of ζ-potential higher than 30 mV (positive or negative) are usually indicators of a good system stability [23]. Primary emulsions presented values of ζ-potential that indicate stable systems, in particular it was of −53 ± 11 mV for A-T-LEO L and −24 ± 1 mV for A-T-LEO H. The negative electrical charge observed can be mainly attributed to the anionic residues of sodium alginate that characterize the continuous phase [23]. Both, the suspension with only alginate and with alginate plus Tween 80, showed a higher negative value of ζ-potential (−71 ± 5 mV and −45 ± 3 mV, respectively). This indicates that the surface electrical charge of the emulsion particles was affected by the partition of polymer chains between the continuous phase and the particle surface that are affected by the droplet size and volume fraction of dispersed phase determining the total interfacial area.

3.2. Film Properties

3.2.1. Microstructure

Previously characterized emulsions were (after being diluted with alginate as the continuous phase) used to produce thin films. The microstructure of the films is the result of the structural arrangement of the different components that affect their physical and mechanical properties. The micrographs of the films' cross-sections obtained by means of FESEM are shown in Figure 3.

Film with alginate only (Figure 3A) showed a homogeneous and compact cryofractured surface, which became thicker (from 50 ± 4 to 62 ± 7 μm) after the application of calcium chloride (Figure 3B) that crosslinked the guluronic residues. It is also possible to notice a layer containing calcium on the top of the film that did not penetrate into the matrix, due to the high degree of cohesion of the polymer chain packing. The structure of films made of sodium alginate emulsions was completely different; the A-T film, in particular, presented a structure characterized by small particles embedded in the matrix that can be attributed to surfactant aggregates (Figure 3C); however, the structure changed when LEO was added (Figure 3E,G). In presence of oil, indeed, the matrix lost its homogeneous structure with the formation of areas of differing densities, due to the destabilization phenomena that occurred during the film drying [24]. No oil droplets were visible, but the lipid entrapment inside the film network filled the porous structure generated inside the matrix. During the film drying step, droplet flocculation, coalescence and creaming occur, which can produce losses of the lipid compounds caused by the steam drag effect at the film surface in line with water evaporation [18]. For A-T based films treated with calcium (Figure 3D), it was possible to notice the formation of a laminar structure, characterized by the assembly of parallel layers, probably separated by Tween 80, which reorganized during drying. Calcium-treated films containing essential oil (Figure 3F,H), became thicker, especially samples with a higher amount of EO (91 ± 16 μm), which had visible oil droplets trapped in the matrix (Figure 3a,b). In both cases, the presence of oil gave rise to a laminar structure, which suggests a greater ability to promote calcium diffusion through the alginate matrix and a more extended crosslinking through the film. Nevertheless, the crosslinked layers were interrupted by the lipid lumps resulting from droplet flocculation and coalescence. The promoted calcium diffusion could be explained by a weakening effect that the lipid compounds exert on the chain attraction forces, allowing calcium mobility inside the polymer network.

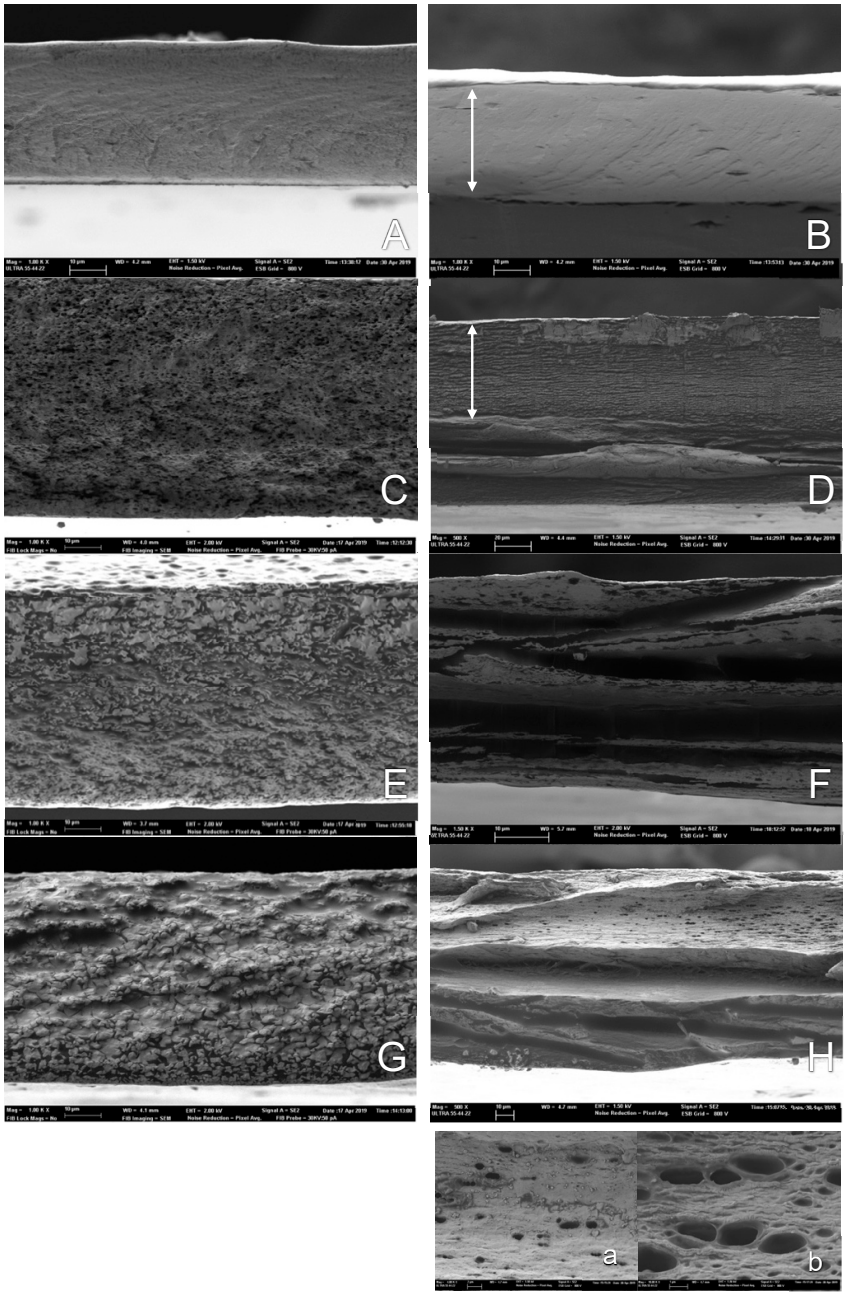

Figure 3. Field Emission Scanning Electron Microscopy (FESEM) micrographs of the obtained films: (**A**) A, (**B**) A-Ca, (**C**) A-T, (**D**) A-T-Ca, (**E**) A-T-LEO L (**F**) A-T-LEO L-Ca (**G**) A-T-LEO H, and (**H**) A-T-LEO H-Ca; a, b—higher magnifications (4,000× and 10,000× respectively) of A-T-LEO H-Ca. White arrows indicate the part of the film cut with a scalpel. All the other samples were cryofractured.

Further information about the physical properties of the obtained films concerned their thermal behavior. Through thermo-gravimetric analysis (TGA), it was possible to evaluate changes (losses of volatile compounds or polymer degradation) in the material associated to the temperature increasing at a constant heating rate. Mass sample changes are related to different events, such as desorption, absorption, sublimation, vaporization, oxidation, etc. Figure 4 depicts the derivative curves (DTGA) obtained from TGA.

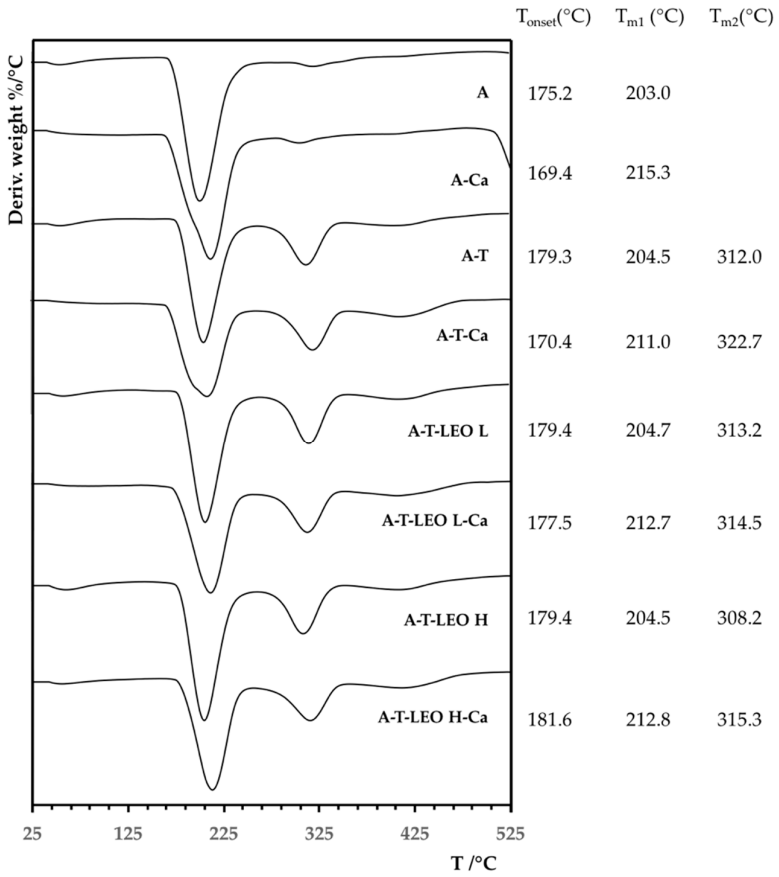

	T_{onset}(°C)	T_{m1} (°C)	T_{m2}(°C)
A	175.2	203.0	
A-Ca	169.4	215.3	
A-T	179.3	204.5	312.0
A-T-Ca	170.4	211.0	322.7
A-T-LEO L	179.4	204.7	313.2
A-T-LEO L-Ca	177.5	212.7	314.5
A-T-LEO H	179.4	204.5	308.2
A-T-LEO H-Ca	181.6	212.8	315.3

Figure 4. Derivative thermo-gravimetric analysis (DTGA) curves of the obtained films. The embedded table gives the values of the onset and peak temperatures.

As can be seen from the figure, alginate, as well as crosslinked films presented a first mass reduction at around 200 °C, associated with the polymer degradation, with the consequent formation of carbonaceous residues and Na_2CO_3, according to Soares and co-workers [25]. Calcium incorporation provoked the shift of the degradation peak to a higher temperature, in agreement with the formation of a more compact structure with greater cohesive forces. The DTGA curves of films made from emulsions showed two peaks, the first (T_{m1}) corresponding to the alginate degradation and a second peak (T_{m2}), also present in the A-T film, which could be associated with the surfactant degradation. As for the alginate film, when calcium was applied to films with LEO, it protected alginate and Tween from thermodegradation, with a shift toward higher values of the peaks corresponding to T_{m1} and T_{m2}.

3.2.2. Moisture Content and Solubility

To better understand the films' behavior and their ability to interact with water, the moisture content (MC) of samples conditioned at a RH of 53% and 25 °C was taken into consideration. Films obtained with only polymer showed MC values of between 10.7–11 g for 100 g of dry film (Table 2), regardless of whether calcium was applied or not. The MC values decreased when the films were obtained from emulsions, reaching the lowest value for sample A-T-LEO H, which can be associated with the presence of hydrophobic compounds or groups that prevented the water adsorption in the matrix [26,27]. Alginate is a biodegradable and hydrophilic polymer, and, in order to expand the possible application fields of its films, a reduction in the solubility is necessary. As expected, films made with pure polymer were totally water soluble and the incorporation of LEO did not significantly modify the film solubility. Other studies on hydrophilic films by Sapper et al. [28] also showed that when the essential oil was directly added to the polymer matrix, no changes in the film

solubility occurred. However, all the films crosslinked with calcium were less soluble than their respective control. In particular, A-Ca and A-T-LEO L-Ca samples had the lowest values of solubility. In every case, the behavior was influenced by the presence of guluronic residues that, with carboxylic groups, can react with calcium ions (typical egg box), or water (like a competitive system).

Table 2. Moisture content (MC as g/100 g dry film), water solubility (S, percentage of soluble solids in the film), water vapor permeability (WVP) and tensile properties (EM, elastic modulus; TS, tensile strength; E, percentage elongation) of the films.

	MC (g/100g)	S (%)	WVP *10^{-9} (g/msPa)	EM (MPa)	TS (MPa)	E (%)	Thickness (μm)
A	10.7 (0.4)^{a,b}	99 (0)^{c}	2.5 (0.2)^{a}	3200 (120)^{d}	80 (5)^{a}	5 (1)^{a}	50 (4)^{a}
A-Ca	11.3 (0.8)^{b}	58 (3.7)^{a}	3.1 (0.6)^{a,b}	3800 (200)^{e}	133 (16)^{b}	7 (2)^{a,b}	62 (7)^{b}
A-T	9.4 (0.2)^{a,b}	95 (2.7)^{c}	3.1 (0.5)^{a}	2500 (98)^{a,b,c}	82 (5)^{a}	11 (1)^{d}	61 (4)^{b}
A-T-Ca	10.1 (0.3)^{a,b}	76 (0)^{a,b,c}	2.8 (0.8)^{a}	2600 (400)^{b,c}	77 (27)^{a}	5 (3)^{a,b}	89 (16)^{c}
A-T-LEO L	9.6 (1.1)^{a,b}	88 (2.4)^{b,c}	2.9 (0.6)^{a,b}	2000 (150)^{a}	70 (7)^{a}	9 (3)^{b,c,d}	66 (6)^{b}
A-T-LEO L-Ca	9.1 (0.6)^{a,b}	65 (7.3)^{a,b}	3.6 (0.5)^{b}	2800 (130)^{c,d}	122 (18)^{b}	11 (3)^{c,d}	83 (12)^{c}
A-T-LEO H	8.9 (1.0)^{a}	98 (2.7)^{c}	2.9 (0.4)^{a}	2400 (90)^{a,b}	70 (7)^{a}	7 (2)^{a,b,c}	64 (6)^{b}
A-T-LEO H-Ca	8.8 (0.9)^{a}	75 (11.4)^{a,b,c}	3.1 (0.4)^{a,b}	2600 (140)^{a,b,c}	72 (16)^{a}	4 (2)^{a}	91 (16)^{c}

Standard deviation is shown in brackets. Any means in the same column followed by different letters are significantly different ($p < 0.05$) for LSD procedure.

3.2.3. Thickness

Film thickness is a crucial parameter for the determination of features, such as mechanical and barrier properties, and it is influenced by the preparation methods, the surface of the plate where the dispersion is cast, the drying time, the solid content and by the phenomena occurring during the drying of the film-forming dispersion. Samples had different thickness values; films obtained from emulsions, in particular, were thicker due to the higher solid content of the film-forming dispersions containing LEO and Tween 80 (Table 2). When calcium chloride was applied, an increase in this parameter was observed, in all likelihood due to the crosslinking effect and the formation of hydrogel during the drying process. During this process, a network starts to be formed as soon as calcium ions find guluronic residues to react with. Pavlath et al. [29] also found an increase in the thickness of alginate films obtained by immersion in solutions of multivalent ion salts and explained that two coupled processes occurred: dissolution of alginate in the solution and the crosslinking between divalent cations and carboxylic groups that made films thicker.

3.2.4. Mechanical Properties

The presence of LEO and the application of calcium influenced the mechanical properties in different ways. This is due to the different microstructure formed, as mentioned above, that depended on both the composition of the film-forming dispersion and its stability during the drying process. Interactions between polymer, essential oil compounds, surface active agent and crosslinker influenced the structure of the film formed. The ratio of G and M residues in alginate also plays an important role in the mechanical and stability properties of alginate films. The values of different mechanical properties are summarized in Table 2 for every sample. Curves of force versus distance obtained in the test curves were transformed into stress (σ) versus Hencky strain (ε_H) and reported in Figure 5. From the curves, it is possible to appreciate a first linear σ–ε_H relationship, associated with the elastic component and a second one indicative of the plastic behavior. Alginate films are hard and strong, with a high value of EM (Elastic Modulus), linked to the film's rigidity and tensile strength (TS) with a moderate value of elongation at break (%E). Different values of tensile properties were reported for alginate films; the TS ranged from 40 to 80 MPa, when conditioned at different % RH and with the presence of plasticizer [30]. The weaker films showed elongation at break from 3 to 5% [31]. When using crosslinking agents, TS values up to 134 MPa were observed for alginate

mulching films [32]. Differences in the tensile properties are also related to the different sources of the polymer, the grade of purity or the extraction method.

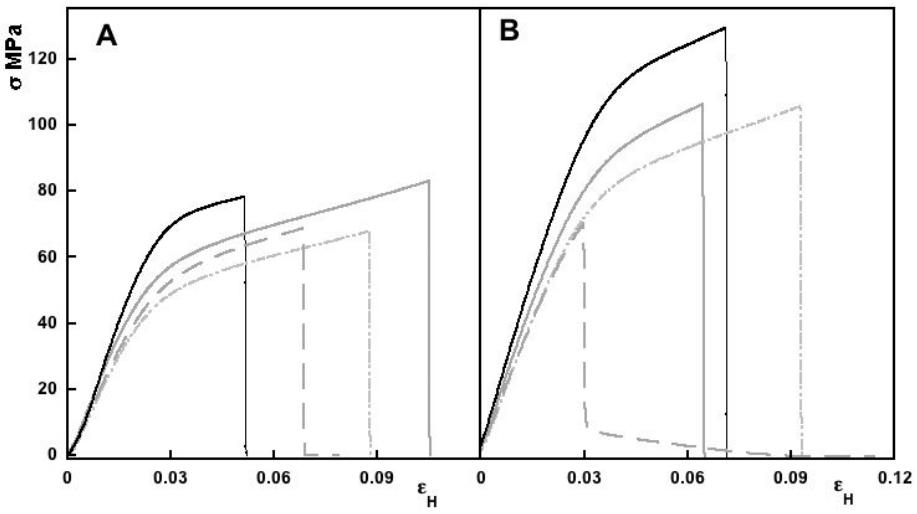

Figure 5. Representative tensile stress (σ)–Hencky strain (ε_H) curves obtained for the different films: A (solid black line), A-T (solid grey line), A-T-LEO L (dashed and dotted grey line) and A-T-LEO H (dashed grey line) without (**A**) and with (**B**) $CaCl_2$.

The outcomes of the mechanical properties revealed that films formed by emulsions or A-T films exhibited a more plastic behavior compared to films made only of alginate. The elastic modulus was indeed higher in the latter case. The rigidity was similar in A and A-T films and was reduced in films made from emulsions, while the films made from emulsions and by A-T suspensions were more resistant to elongation compared to films made of pure alginate. This can be attributed to the fact that all the added components increased the chain mobility and reduced the inter-chain forces, thus enhancing the percentage of elongation at break. In particular, LEO compounds could favor the sliding of the chains during film stretching [33]. This behavior concurs with that observed by other authors [34–36]. When calcium was applied, a significant increase ($p < 0.05$) in the tensile strength was clearly observed for every crosslinked sample, as was a reduction in the elongation at the break. Costa el at. [37] also observed the same effect on A-Ca films. High values of TS are usually due to the presence of H bounds or crosslinking between the chain of the polymer as promoted by calcium application [32,38]. The application of calcium during the drying step produced films in which the final structure was a compromise between the instantaneous formation of an insoluble complex and the dissolution of alginate in the matrix. Therefore, regions with a high density of crosslinking and others with a low density could be expected. This would explain the observed variability in the mechanical properties.

3.2.5. Barrier Properties

Water vapor permeability (WVP) is related to the diffusion and solubility of water molecules through the film section and high values of WVP are usually recorded for hydrophilic films. The water vapor transfer process is conditioned by the hydrophilic/hydrophobic ratio of the film components and, as previously mentioned, the film's microstructure also influenced the barrier properties. WVP values of every sample are shown in Table 2. In general, for the obtained films, WVP was scarcely affected by the film composition or calcium application. The incorporation of essential oil did not significantly modify the WVP of the films, while calcium application seemed to slightly promote WVP, although no significant differences were observed between the values of the calcium treated films and the corresponding control sample. This is because the formation of an emulsion as well as the application of calcium could change the matrix and create pores or other channels that

allowed water molecules to pass through the polymer matrix [39]. However, some authors [30] reported how increasing the calcium concentration led to an enhancement in the water vapor barrier properties up to a maximum value, and higher amounts of calcium lead to poorer water vapor barrier properties. As concerns the effect of essential oils, some studies demonstrated that their addition improved film properties, such as moisture content and water vapor permeability [40,41], whereas others reported that these properties were negatively influenced by the different structural arrangement that creates channels or fractures leading to a worsening of the barrier properties [36,39].

3.2.7. Optical Properties

The optical properties of the films affect the appearance and quality of the foodstuff on which they are applied, having a great impact on consumer acceptability [24]. Color changes could usually be a sign of lipid oxidation that affects the quality of foods. Although all of the films studied appeared transparent, especially that made with pure alginate, samples obtained from emulsions were slightly opalescent. The addition of LEO at higher concentrations provided the film with a yellowish color. Table 3 reports the L*, C_{ab}*, h_{ab}*, WI and ΔE values (lightness, chrome, hue, whiteness index and total color difference respectively) and internal transmittance values for every film.

Table 3. Lightness L*, chrome C_{ab}*, hue h_{ab}*, whiteness index (WI), total color difference (**ΔE**) values and internal transmittance (Ti) at 450 nm of developed films.

Sample	L*	C_{ab}*	h_{ab}*	Ti 450 nm	WI	ΔE
A	83.6 (0.9)^{d}	9.0 (0.6)^{a,b,c}	89.3 (0.9)^{a,b}	0.842 (0.003)^{f}	81 (1)^{d}	-
A-Ca	80.0 (1.6)^{b,c}	8.4 (1.0)^{a,b}	89.8 (1.8)^{a,b}	0.838 (0.006)^{e,f}	78 (1)^{b,c}	3.8 (1.6)^{a}
A-T	82.0 (1.3)^{c,d}	10.7 (1.0)^{c}	89.3 (0.8)^{a,b}	0.826 (0.008)^{d,e}	79 (1)^{c,d}	2.7 (0.8)^{a}
A-T-Ca	77.6 (2.1)^{a,b}	7.1 (0.8)^{a}	94.5 (2.3)^{c}	0.798 (0.012)^{b,c}	76(2)^{b,c}	6.9 (1.7)^{c}
A-T-LEO L	79.6 (1.6^{b,c}	12.9 (0.7)^{d}	88.0 (0.9)^{a}	0.811 (0.007)^{c,d}	76 (1)^{b}	5.8 (0.8)^{b,c}
A-T-LEO L-Ca	78.7 (4.1)^{a,b,c}	10.1 (1.9)^{b,c}	91.0 (2.1)^{b}	0.782 (0.015)^{b}	76 (3)^{b}	4.2 (1.5) ^{a,b}
A-T-LEO H	77.4 (1.5)^{a,b}	17.1 (1.6)^{e}	89.4 (1.4)^{a,b}	0.810 (0.007)^{c,d}	72 (1)^{a}	10.5 (0.9)^{d}
A-T-LEO H-Ca	75.3 (2.0)^{a}	15.1 (1.7)^{e}	90 (1.6)^{a,b}	0.763 (0.010)^{a}	71 (1)^{a}	10.6 (1.0)^{d}

Average values and standard deviations in brackets. Any means in the same column followed by different letters are significantly different ($p < 0.05$) for LSD procedure.

The lightness value was higher for films made of pure alginate. These values tend to decrease when emulsions were used to produce films, in particular for the highest amount of LEO. Moreover, for a determined film composition, calcium application provoked a decrease in the L* value. Hue values were less affected than chrome values. C_{ab}* increased in the films containing LEO due to the natural color of the oil, while the opposite behavior was observed for the whiteness index (WI), which decreased in samples containing LEO. Nevertheless, it is not affected by the application of calcium. The differences in color parameters for the films were also determined through the ΔE values (total color difference) calculated with respect to alginate films. As expected from the individual values of color parameters, the highest ΔE was obtained for film with the highest amount of essential oil. The spectral distribution of internal transmittance is shown in Figure 5. Films with essential oil exhibit less internal transmittance at lower values of wavelength due to the selective light absorption of oil compounds. As also observed by Sanchez-Gonzalez et al. [42], the transparency of hydrophilic films with EO decreases due to the presence of a dispersed phase in the matrix, with different refractive index, which promotes light dispersion.

Likewise, compared to the respective control, the application of calcium gave rise to more opaque films. The opacity effect of calcium application was more intense in films containing surfactant and LEO, coherent with the greater penetration of the ion into the network and the progress of crosslinking in the internal part of the film, as deduced from the microstructural observations. The heterogeneous microstructure of the films crosslinked with calcium would provoke greater light dispersion and higher degree of opacity.

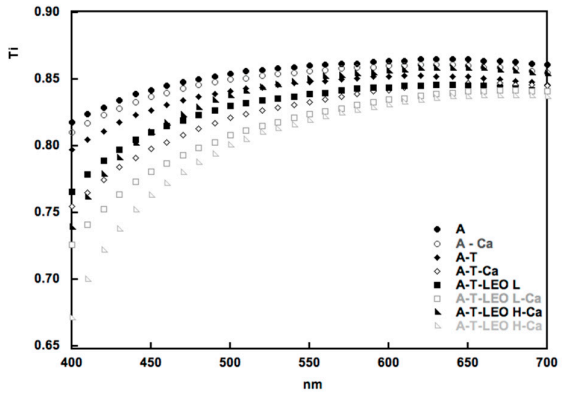

Figure 5. Spectral distribution of internal transmittance (Ti) of films with and without calcium chloride.

Finally, considering all the outcomes of this study, some aspects can be highlighted. The decrease in the film's solubility caused by calcium is correlated with an increase in the tensile strength, underlying the fact that low values of solubility and greater resistance to an external stress are related to the formation of a crosslinked structure through the action of calcium in the guluronic cavities of the polymer network. A further correlation was recognized between the sample microstructure and the optical properties of the films. These become less transparent, darker and with a more saturated color when they contained essential oil, while calcium application induced more opacity. However, the cross-linked structures did not exhibit an improved barrier capacity against water vapor.

4. Conclusions

Reinforced films of alginate, containing or not emulsified lemongrass essential oil, were obtained by spraying calcium chloride onto their surface. The film-forming emulsions were stabilized by Tween 80, exhibiting a particle size affected by the surfactant:oil ratio and negative ζ-potential values. Calcium diffusion through the film was favored in emulsified formulations, although the discontinuities introduced by the oil in the polymer network gave rise to weaker films, with lower elastic modulus and tensile strength at break. The crosslinking caused by calcium ions reduced the water solubility of the films, promoted the film's opacity and increased the temperature of the polymer thermal degradation. These effects were more pronounced in films containing essential oil, in line with the greater diffusion of the cation in the less compact, discontinuous oil–polymer matrix. Then, the proposed method of film production based on alginate emulsions and calcium spraying could be a suitable way to extend the field of application of polymeric edible films.

Author Contributions: Conceptualization, M.C. and A.C.; methodology, M.C.; investigation, M.C.; data curation, M.C and F.C..; writing—original draft preparation, M.C. and F.C.; writing—review and editing, M.C., F.C. and A.C.

Funding: This research was funded by the Ministerio de Economía y Competitividad (MINECO) of Spain, through the project AGL2016-76699-R.

Conflicts of Interest: The authors declare no conflict of interest

References

1. Rossi, M.; Passeri, D.; Sinibaldi, A.; Angjellari, M.; Tamburri, E.; Sorbo, A.; Carata, E.; Dini, L. Nanotechnology for Food Packaging and Food Quality Assessment. In *Advances in Food and Nutrition Research*, Elsevier: Amsterdam, The Netherlands, 2017; Vol. 82, pp. 149–204.
2. Risch, S.J. New Developments in Packaging Materials. ACS Publications: Washington, DC, USA, 2000.
3. Shit, S.C.; Shah, P.M. Edible polymers: Challenges and opportunities. *J. Polym.* **2014**, *2014*.
4. Embuscado, M.E.; Huber, K.C. *Edible Films and Coatings for Food Applications*; Springer-Verlag: New York, NY, USA, 2009; Vol. 9.

5. Donhowe, I.G.; Fennema, O. Edible films and coatings: Characteristics, formation, definitions, and testing methods. *Edible Coatings Films Improv. Food Qual.* **1994**, 1–24.
6. Tavassoli-Kafrani, E.; Shekarchizadeh, H.; Masoudpour-Behabadi, M. Development of edible films and coatings from alginates and carrageenans. *Carbohydr. Polym.* **2016**, *137*, 360–374.
7. Cofelice, M.; Cuomo, F.; Lopez, F. Rheological Properties of Alginate–Essential Oil Nanodispersions. *Colloids Interfaces* **2018**, *2*, 48.
8. Cuomo, F.; Lopez, F.; Ceglie, A.; Maiuro, L.; Miguel, M.G.; Lindman, B. pH-responsive liposome-templated polyelectrolyte nanocapsules. *Soft Matter* **2012**, *8*, 4415–4420.
9. Cuomo, F.; Cofelice, M.; Lopez, F. Rheological Characterization of Hydrogels from Alginate-Based Nanodispersion. *Polymers* **2019**, *11*, doi:doi:10.3390/polym11020259.
10. Burt, S. Essential oils: Their antibacterial properties and potential applications in foods—a review. *Int. J. Food Microbiol.* **2004**, *94*, 223–253.
11. Donsi, F.; Ferrari, G. Essential oil nanoemulsions as antimicrobial agents in food. *J. Biotechnol.* **2016**, *233*, 106–120.
12. Liakos, I.; Grumezescu, A.; Holban, A.; Florin, I.; D'Autilia, F.; Carzino, R.; Bianchini, P.; Athanassiou, A. Polylactic acid—lemongrass essential oil nanocapsules with antimicrobial properties. *Pharmaceuticals* **2016**, *9*, 42.
13. Mbili, N.C.; Opara, U.L.; Lennox, C.L.; Vries, F.A. Citrus and lemongrass essential oils inhibit Botrytis cinerea on 'Golden Delicious','Pink Lady'and 'Granny Smith'apples. *J. Plant Dis. Prot.* **2017**, *124*, 499–511.
14. Azarakhsh, N.; Osman, A.; Ghazali, H.M.; Tan, C.P.; Adzahan, N.M. Lemongrass essential oil incorporated into alginate-based edible coating for shelf-life extension and quality retention of fresh-cut pineapple. *Postharvest Boil. Technol.* **2014**, *88*, 1–7.
15. Cofelice, M.; Lopez, F.; Cuomo, F. Quality Control of Fresh-Cut Apples after Coating Application. *Foods* **2019**, *8*, 189.
16. Valencia-Sullca, C.; Jiménez, M.; Jiménez, A.; Atarés, L.; Vargas, M.; Chiralt, A. Influence of liposome encapsulated essential oils on properties of chitosan films. *Polym. Int.* **2016**, *65*, 979–987.
17. Astm. Standard test method for tensile properties of thin plastic sheeting. *Annu. Book Am. Stand. Test. Methods* **2001**, 162–170.
18. Astm. Standard test methods for water vapour transmission of materials. *Annu. Book ASTM* **1995**, 406–413.
19. McHugh, T.H.; Avena-Bustillos, R.; Krochta, J. Hydrophilic edible films: Modified procedure for water vapor permeability and explanation of thickness effects. *J. Food Sci.* **1993**, *58*, 899–903.
20. Hutchings, J.B. Instrumental specification. In *Food colour and appearance*, Springer: 1999; pp. 199–237.
21. Dawson, R.; Elliott, D.; Elliott, W. Jones KM: Data for Biochemical Research. Oxford: Clarendon Press: 1986.
22. Rao, J.; McClements, D.J. Formation of flavor oil microemulsions, nanoemulsions and emulsions: Influence of composition and preparation method. *J. Agric. Food Chem.* **2011**, *59*, 5026–5035.
23. McClements, D.J. Food emulsions: Principles, practices, and techniques; CRC press: 2015.
24. Atarés, L.; Chiralt, A. Essential oils as additives in biodegradable films and coatings for active food packaging. *Trends Food Sci. & Technol.* **2016**, *48*, 51–62.
25. Soares, J.d.P.; Santos, J.; Chierice, G.O.; Cavalheiro, E. Thermal behavior of alginic acid and its sodium salt. *Eclética Quím.* **2004**, *29*, 57–64.
26. Hosseini, M.H.; Razavi, S.H.; Mousavi, S.M.A.; Yasaghi, S.A.S.; Hasansaraei, A.G. Improving antibacterial activity of edible films based on chitosan by incorporating thyme and clove essential oils and EDTA. *J. Appl. Sci.* **2008**, *8*, 2895–2900.
27. Riquelme, N.; Herrera, M.L.; Matiacevich, S. Active films based on alginate containing lemongrass essential oil encapsulated: Effect of process and storage conditions. *Food Bioprod. Process.* **2017**, *104*, 94–103.
28. Sapper, M.; Wilcaso, P.; Santamarina, M.P.; Roselló, J.; Chiralt, A. Antifungal and functional properties of starch-gellan films containing thyme (Thymus zygis) essential oil. *Food Control.* **2018**, *92*, 505–515.
29. Pavlath, A.; Gossett, C.; Camirand, W.; Robertson, G. Ionomeric films of alginic acid. *J. Food Sci.* **1999**, *64*, 61–63.
30. Olivas, G.I.; Barbosa-Cánovas, G.V. Alginate–calcium films: Water vapor permeability and mechanical properties as affected by plasticizer and relative humidity. *LWT-Food Sci. Technol.* **2008**, *41*, 359–366.
31. Siracusa, V.; Romani, S.; Gigli, M.; Mannozzi, C.; Cecchini, J.; Tylewicz, U.; Lotti, N. Characterization of Active Edible Films based on Citral Essential Oil, Alginate and Pectin. *Materials* **2018**, *11*, 1980.

32. Liling, G.; Di, Z.; Jiachao, X.; Xin, G.; Xiaoting, F.; Qing, Z. Effects of ionic crosslinking on physical and mechanical properties of alginate mulching films. *Carbohydr. Polym.* **2016**, *136*, 259–265.
33. Bonilla, J.; Atarés, L.; Vargas, M.; Chiralt, A. Effect of essential oils and homogenization conditions on properties of chitosan-based films. *Food Hydrocoll.* **2012**, *26*, 9–16.
34. Atarés, L.; Pérez-Masiá, R.; Chiralt, A. The role of some antioxidants in the HPMC film properties and lipid protection in coated toasted almonds. *J. Food Eng.* **2011**, *104*, 649–656.
35. Benavides, S.; Villalobos-Carvajal, R.; Reyes, J. Physical, mechanical and antibacterial properties of alginate film: Effect of the crosslinking degree and oregano essential oil concentration. *J. Food Eng.* **2012**, *110*, 232–239.
36. Pranoto, Y.; Salokhe, V.M.; Rakshit, S.K. Physical and antibacte rial properties of alginate-based edible film incorporated with garlic oil. *Food Res. Int.* **2005**, *38*, 267–272.
37. Costa, M.J.; Marques, A.M.; Pastrana, L.M.; Teixeira, J.A.; Sillankorva, S.M.; Cerqueira, M.A. Physicochemical properties of alginate-based films: Effect of ionic crosslinking and mannuronic and guluronic acid ratio. *Food Hydrocoll.* **2018**, *81*, 442–448.
38. Rhim, J.-W. Physical and mechanical properties of water resistant sodium alginate films. *LWT-Food Sci. Technol.* **2004**, *37*, 323–330.
39. Baek, S.-K.; Kim, S.; Song, K. Characterization of Ecklonia cava Alginate Films Containing Cinnamon Essential Oils. *Int. J. Mol. Sci.* **2018**, *19*, 3545.
40. Abdollahi, M.; Rezaei, M.; Farzi, G. A novel active bionanocomposite film incorporating rosemary essential oil and nanoclay into chitosan. *J. Food Eng.* **2012**, *111*, 343–350.
41. Tongnuanchan, P.; Benjakul, S.; Prodpran, T. Properties and antioxidant activity of fish skin gelatin film incorporated with citrus essential oils. *Food Chem.* **2012**, *134*, 1571–1579.
42. Sánchez-González, L.; González-Martínez, C.; Chiralt, A.; Cháfer, M. Physical and antimicrobial properties of chitosan–tea tree essential oil composite films. *J. Food Eng.* **2010**, *98*, 443–452.